PHYSICAL REVIEW A VOLUME 22, NUMBER 1 JULY 1980

Atomic polarizability in negative-ion photodetachment

S. Watanabe and Chris H. Greene
Department of Physics, University of Chicago, Chicago, Illinois 60637

(Received 17 December 1979)

The influence of a strong atomic polarizability on photodetachment processes is isolated. In a model study of K^- photodetachment near the $4p_{1/2}$, $4p_{3/2}$ levels of K, the polarizability ($\alpha_{4p} \simeq 600a_0^3$) is shown to cause a striking energy dependence of the parameters which determine the cross section. This study extends the effective range theory of O'Malley, Spruch, and Rosenberg to a broader energy range and to multichannel systems. An appendix provides a derivation of the polarization potential (and correction terms) starting from the electron-atom close-coupling equations, showing some new features.

I. INTRODUCTION

The photodetachment cross sections of all the alkali negative ions (except Fr^-) have been accurately measured in recent years.[1,2] All of these measurements have shown autodetaching resonances near the first excited state of the alkali atom. In Cs^-, for example, a narrow window-type resonance of width ~2 meV was found just below each of the two fine-structure levels $6p\ ^2P_{1/2,3/2}$. The geometry of these negative ions is simple, consisting of two electrons outside a spherically symmetric closed-shell core, but the fine-structure dynamics remains quite complicated by the interplay of electron correlation and spin-orbit interaction.

Lee first interpreted the Cs^- results semiempirically.[3] He expressed the photodetachment cross section in terms of two dipole matrix elements D_α and of their derivatives with respect to the energy, and in terms of six energy-independent elements of a 4×4 reaction matrix K_{ij}. Lee successfully fitted his ten-parameter expression to the observed total cross section, obtaining semiempirical values for the K_{ij}, D_α, and dD_α/dE. (Actually, only nine of the parameters were determined, since the experimental results were not measured absolutely.) While this fitting procedure successfully reproduced the photodetachment cross section using an energy-independent reaction matrix, close-coupling calculations by Moores and Norcross[4(b)] obtained K-matrix elements which varied rapidly (e.g., by more than a factor of two over the 550 cm^{-1} interval between the atomic fine-structure levels $^2P_{1/2,3/2}$). This apparent discrepancy has been partially clarified by Norcross and Taylor,[4(a)] who found that their calculated scattering matrix S_C was related to Lee's fitted scattering matrix S_F by a transformation

$$S_C = e^{i\delta} S_F e^{i\delta}\,, \tag{1.1}$$

where δ is a diagonal matrix (in ij), whose elements vary with energy. The photodetachment cross sections are invariant under this transformation of S_C, so it is not surprising that Lee successfully fitted the data with an energy-independent reaction matrix.

While the explanation of Norcross and Taylor[4(a)] has clarified the mathematical ambiguity of Lee's semiempirical approach, it does not provide a systematic method for dealing with the strong energy dependence of K. This energy dependence, which Norcross and Taylor[4(a)] attributed to the polarizability of the excited atom, particularly hampered their calculation of cross sections. In the present paper we isolate the effect of the atomic polarizability and calculate it separately, thereby extending the single-channel effective range theory of O'Malley, Spruch, and Rosenberg[5] (OSR) to multichannel systems. As shown in the preceding article[6] [see Eq. (2.27)], a major portion of the energy dependence does indeed take the form of a phase shift δ as in (1.1). But in general, the induced energy dependence is more complicated. An initial study of this problem was made long ago by O'Malley.[7] The generalized theoretical framework of quantum-defect theory presented recently[8] permits us to write the reaction matrix in terms of two separate groups of parameters: slowly varying ones representing the effect of short-range interactions, and rapidly varying parameters characterizing the long-range field alone. These latter parameters depend only on the polarizability α_i, orbital angular momentum l_i, and the energy ϵ_i in each dissociation channel i. As an application, we then show that the strong polarizability of the excited alkali atom ($\alpha \sim 600a_0^3$ for the potassium $4p$ state) accounts for the energy dependence of the reaction matrices calculated by Norcross and Taylor[4(a)] (see Figs. 5–7 in Sec. III).

In the Appendix we show how the long-range close-coupling equations approximately reduce to a set of uncoupled single-channel Schrödinger equations with a polarization potential $-\alpha_i/2r^4$ in each channel i. Though this problem has been studied extensively in the past, we point out some new features which have emerged from our analysis. Our result for the energy-dependent r^{-6} correction term differs from previous derivations[9,10] in sign and magnitude.

II. QUANTUM-DEFECT PARAMETERS FOR THE POLARIZATION FIELD

In the absence of quadrupole moments, the polarization field is the dominant long-range field for the compound of an electron and a nonpolar neutral atom (or molecule). Its potential (in a.u.) is, to a good approximation, proportional to r^{-4} (Ref. 11), i.e.,

$$V_{\text{pol}}(r) = -\alpha/2r^4\,, \tag{2.1}$$

where α is the atomic polarizability of the neutral atom in a given state (see the Appendix). The Schrödinger equation of an electron in this field is

$$\left(-\tfrac{1}{2}\frac{d^2}{dr^2} + \frac{l(l+1)}{2r^2} - \frac{f^2}{2r^4} - \frac{k^2}{2}\right) f(\epsilon, l; r) = 0\,, \tag{2.2}$$

where we have set $\alpha = f^2$. This equation can be solved analytically using the Mathieu functions. Here we utilize these functions for mathematical convenience and defer until the end of this section the discussion of the energy dependence of the quantum-defect theory (QDT) parameters to be obtained below.

It has been shown by Vogt and Wannier[12] that the functions $r^{1/2}M_{\pm\tau}[\ln[(k/f)^{1/2}r]]$ satisfy Eq. (2.1) where $M_{\pm\tau}[\ln[(k/f)^{1/2}r]]$ are the Mathieu functions of order $\pm\tau$. These functions were previously used by OSR[5] in their effective range theory for an r^{-4} potential. The functions $M_{\pm\tau}[\ln x]$ themselves satisfy the equation

$$\left(x^2\frac{d^2}{dx^2} + x\frac{d}{dx} - (l+\tfrac{1}{2})^2 + kf(x^2 + x^{-2})\right) M_{\pm\tau}[\ln x] = 0\,. \tag{2.3}$$

The radial variable r is related to the scaled variable x by $x = (k/f)^{1/2}r$, while τ is a function of l and kf. The parameter τ is related to an infinite Hill's determinant Δ by $\sin^2(\pi\tau/2) = \Delta/2$, and plays the role of an indicial-type parameter. A further change of variables $x = e^{\phi}$ reduces Eq. (2.3) to the standard form of the Mathieu equation:

$$\left(\frac{d^2}{d\phi^2} - (l+\tfrac{1}{2})^2 + 2kf\cosh(2\phi)\right) M_{\pm\tau}[\phi] = 0\,. \tag{2.4}$$

It should be noted that Eq. (2.2) has irregular singularities at $x = 0$ and $x = \infty$; the series representation of the solutions $M_{\pm\tau}[\ln x]$ is given by

$$M_{\pm\tau}[\ln x] = \frac{1}{K^{\pm}} \sum_{n=-\infty}^{\infty} C_n(\tau) x^{\pm(\tau+2n)}\,. \tag{2.5}$$

Here $C_0(\tau) = 1$ as in Ref. 13. The constants $K^{\pm}$ normalize $M_{\pm\tau}[\ln x]$ as in the corresponding functions of OSR and are defined by Eq. (17) of Ref. 13. Equation (2.3) has an obvious symmetry under $x \to 1/x$. From Eq. (2.5),

$$M_{+\tau}[\ln(1/x)] = m(\tau) M_{-\tau}[\ln x]\,, \tag{2.6}$$

where $m(\tau) = M_{+\tau}(0)/M_{-\tau}(0) = K^-/K^+$. The parameter $m = m(\tau)$ plays an important role in connecting the solutions corresponding to the two limiting cases $x \to 0$ and $x \to \infty$. The determination of τ and $C_n(\tau)$ $(-\infty \leq n \leq \infty)$ is discussed by Morse and Feshbach.[14] A method for computing m as well as τ and $C_n(\tau)$ is detailed in Ref. 13. The Hill's determinant Δ is an oscillatory function of kf. Its amplitude and the spacing between its zeros increase monotonically as kf increases. For small values of kf, the parameter Δ lies between 0 and 2, and τ is real. When kf is large, the solution to the equation $\sin^2(\pi\tau/2) = \Delta/2$ almost always takes the form $\tau = \text{integer} + i\mu$ (μ real). In this case m is also complex, and the Mathieu functions $M_{\pm\tau}[\ln x]$ are complex valued.

Suitable linear combinations of $r^{1/2}M_{\pm\tau}[\ln(k/f)^{1/2}r]$ yield real standing-wave solutions for $\epsilon > 0$. Solutions to Eq. (2.1) which are real and analytic functions of the energy, have been given by OSR. Following the convention of Greene, Fano, and Strinati (GFS),[8] we denote the base pair which is analytic in energy at all finite r by (f^0, g^0). The base pair (f^0, g^0) differs from the solutions (3.12) and (3.13) in OSR only by a multiplicative constant $(-1)^l(2f/\pi)^{1/2}$. This base pair is normalized near $r = 0$ independently of the energy ϵ, and its Wronskian is $W_\epsilon(f^0, g^0) = 2/\pi$. We define the base pair (f^0, g^0) explicitly as follows:

$$f^0(\epsilon, l; r) = \frac{r^{1/2}}{\cos 2\delta}\left((-1)^l m \cos\delta M_{-\tau}[\ln x] + \frac{1}{m}\sin\delta M_{\tau}[\ln x]\right), \tag{2.7a}$$

$$g^0(\epsilon, l; r) = \frac{r^{1/2}}{\cos 2\delta}\left((-1)^l m \sin\delta M_{-\tau}[\ln x] + \frac{1}{m}\cos\delta M_{\tau}[\ln x]\right), \tag{2.7b}$$

where $\delta = \frac{1}{2}\pi(\tau - l - \frac{1}{2})$ as in OSR.

The small-r and large-r forms of (f^0, g^0) are equivalent to those of OSR. At small r,

$$f^0(\epsilon,l;r) \xrightarrow[r\to 0]{} (2/\pi f)^{1/2}(-1)^l r\sin(f/r-l\pi/2)\,, \tag{2.8a}$$

$$g^0(\epsilon,l;r) \xrightarrow[r\to 0]{} (2/\pi f)^{1/2}(-1)^l r\cos(f/r-l\pi/2)\,, \tag{2.8b}$$

for both $\epsilon>0$ and $\epsilon<0$. At large r, we have

$$f^0(\epsilon,l;r) \xrightarrow[r\to\infty]{} (2/\pi k)^{1/2}[\eta_1\cos(kr-l\pi/2) + \eta_2\sin(kr-l\pi/2)]\,, \tag{2.9a}$$

$$g^0(\epsilon,l;r) \xrightarrow[r\to\infty]{} (2/\pi k)^{1/2}[\eta_3\cos(kr-l\pi/2) + \eta_4\sin(kr-l\pi/2)]\,, \tag{2.9b}$$

when $\epsilon>0$, and

$$f^0(\epsilon,l;r) \xrightarrow[r\to\infty]{} (\nu/2\pi)^{1/2} \times(\mathrm{Re}\{(\eta_1-i\eta_2)\exp[-i\tfrac{1}{2}\pi(l+\tfrac{1}{2})]\}e^{-r/\nu} + \{(\eta_1+i\eta_2)\exp[i\tfrac{1}{2}\pi(l-\tfrac{1}{2})]\}e^{r/\nu}) \tag{2.10a}$$

$$g^0(\epsilon,l;r) \xrightarrow[r\to\infty]{} (\nu/2\pi)^{1/2} \times(\mathrm{Re}\{(\eta_3-i\eta_4)\exp[-i\tfrac{1}{2}\pi(l+\tfrac{1}{2})]\}e^{-r/\nu} + \{(\eta_3+i\eta_4)\exp[i\tfrac{1}{2}\pi(l-\tfrac{1}{2})]\}e^{r/\nu})\,, \tag{2.10b}$$

when $\epsilon<0$. Here we have set

$$\left.\begin{matrix}\eta_1\\ \eta_4\end{matrix}\right\} = \tfrac{1}{2}\left[\left(m+\frac{1}{m}\right)\pm\left(m-\frac{1}{m}\right)\frac{1}{\cos 2\delta}\right]\,, \tag{2.11a}$$

$$\left.\begin{matrix}\eta_2\\ \eta_3\end{matrix}\right\} = \pm\tfrac{1}{2}(1/m-m)\tan 2\delta\,. \tag{2.11b}$$

(Note, $\eta_1\eta_4-\eta_2\eta_3=1$.) The coefficients of $e^{-r/\nu}$ are not automatically real due to the occurrence of the Stokes phenomenon as discussed in the Appendix of GFS. The real parts of the coefficients of $e^{-r/\nu}$ were thus taken explicitly for both f^0 and g^0. The solutions (f^0,g^0) oscillate rapidly near $r=0$ where V_{pol} is large and negative. The rapid oscillations near $r=0$ have no physical consequences as the r^{-4} potential never holds all the way down to $r=0$ in actual problems, just as for the attractive r^{-2} field discussed in GFS. The coefficients $m+1/m$ and $m-1/m$ are, respectively real and purely imaginary[15] in the range of positive energies when τ equals an integer $+i\mu$; hence, the η_i are all real as they should be.

In quantum-defect theory the relationship between solutions normalized near $r=0$ and those energy normalized at $r=\infty$ is expressed in terms of standard parameters. The energy normalized solution f is chosen to be proportional to f^0. The other energy normalized solution g oscillates 90° out of phase asymptotically,

$$f(\epsilon,l;r) \xrightarrow[r\to\infty]{} (2/\pi k)^{1/2}\sin[kr-i\zeta\ln r + \eta(k,l)]\,, \tag{2.12a}$$

$$g(\epsilon,l;r) \xrightarrow[r\to\infty]{} -(2/\pi k)^{1/2}\cos[kr-i\zeta\ln r + \eta(k,l)]\,, \tag{2.12b}$$

where ζ is i/k for the Coulomb field, but vanishes otherwise. (Cf. Sec. II D of GFS.) For $\epsilon<0$, these solutions assume the form

$$f(\epsilon,l;r) = (\nu/\pi)^{1/2}[\sin\beta(\nu,l)D^{-1}f^- - \cos\beta(\nu,l)Df^+]\,, \tag{2.13a}$$

$$g(\epsilon,l;r) = -(\nu/\pi)^{1/2}[\cos\beta(\nu,l)D^{-1}f^- + \sin\beta(\nu,l)Df^+]\,, \tag{2.13b}$$

where the pair (f^+,f^-) is composed of the outgoing and incoming waves for $\epsilon>0$ and $f^{\pm}(\epsilon,l;r)\xrightarrow[r\to\infty]{} e^{\mp r/\nu}r^{\pm\zeta}$ when $\epsilon<0$. The relationship between the base pairs (f^0,g^0) and (f,g) are expressed by the linear transformation

$$\begin{pmatrix} f\\ g\end{pmatrix} = \begin{pmatrix} B^{1/2} & 0\\ B^{-1/2}\mathcal{G} & B^{-1/2}\end{pmatrix}\begin{pmatrix} f^0\\ g^0\end{pmatrix} \quad \epsilon>0 \tag{2.14a}$$

$$\begin{pmatrix} f\\ g\end{pmatrix} = \begin{pmatrix} A^{1/2} & 0\\ A^{-1/2}\mathcal{G} & A^{-1/2}\end{pmatrix}\begin{pmatrix} f^0\\ g^0\end{pmatrix} \quad \epsilon<0\,. \tag{2.14b}$$

Our task is to derive expressions for these QDT parameters B, η, A, β, D, and $\mathcal{G}$ in terms of m and τ by comparing the asymptotic forms of (f^0,g^0) and (f,g). From Eqs. (2.9), (2.12), and (2.14), B and η are obtained by inspection. The negative-energy parameters A and $\mathcal{G}$ depend on the choice of $\beta(\nu,l)$ and D. The parameter D scales the coefficients of f^+ and f^- to comparable magnitudes so as to minimize the energy dependence of the phase-shift parameter $\beta(\nu,l)$. The parameter $\beta(\nu,l)$ must be constrained to yield the alternating zeros of the coefficients of f^+ and f^- (in the expansion of f^0), and must further be interpolated smoothly between them. This then makes the energy dependence of D smooth. General procedures for specifying $\beta(\nu,l)$ and D were left ambiguous in GFS. We choose a particular convention in order to satisfy the above properties of $\beta(\nu,l)$ and D. Here we set

$$\beta(\nu, l) = (l+1)\pi \pm \arg\{(\eta_1 - i\eta_2)\exp[-i\tfrac{1}{2}\pi(l+\tfrac{1}{2})]\}, \qquad (2.15)$$

where a suitable choice of the branch is implied to be made consistently with the signs of $\mathrm{Re}\{(\eta_1 - i\eta_2)\exp[-i\frac{1}{2}\pi(l+1/2)]\}$ and $(\eta_1 + i\eta_2)\exp[i\frac{1}{2}\pi(l-1/2)]$, so that the parameter D below is real and positive. The first term $(l+1)\pi$ is the threshold value of β (modulo 2π). Correspondingly, we set

$$D^2 = \frac{|\eta_1 - i\eta_2|\sin\beta(\nu, l)}{(\eta_1 + i\eta_2)\exp[i\frac{1}{2}\pi(l-\frac{1}{2})]} \geqslant 0. \qquad (2.16)$$

At $f/\nu = (f/\nu)_b$ where the denominator vanishes, $\sin\beta$ also vanishes; and D is defined by its limit as f/ν approaches $(f/\nu)_b$. The parameter $\mathcal{G}(\nu, l)$ is obtained uniquely from Eqs. (2.10), (2.13), and (2.14) once B, A, η, β, and D are fixed. Thus we have

$$A^{-1}(\nu, l) = \tfrac{1}{2}[(\eta_1 + i\eta_2)^2\exp[i\pi(l-\tfrac{1}{2})]D^2 + (\mathrm{Re}\{(\eta_1 - i\eta_2)\exp[-\tfrac{1}{2}i\pi(l+\tfrac{1}{2})]\})^2 D^{-2}],$$

$$B^{-1}(k, l) = \eta_1^2 + \eta_2^2,$$

$$\beta(\nu, l) = (l+1)\pi \pm \arg\{(\eta_1 - i\eta_2)\exp[-\tfrac{1}{2}i\pi(l+\tfrac{1}{2})]\}$$

[Threshold value $\equiv (l+1)\pi$, modulo 2π],

$$\eta(k, l) = \arctan(\eta_1/\eta_2) - \tfrac{1}{2}l\pi,$$

$$D^2 = |\eta_1 - i\eta_2|\sin\beta(\nu, l)/\{(\eta_1 + i\eta_2)\exp[\tfrac{1}{2}i\pi(l-\tfrac{1}{2})]\},$$

$$\mathcal{G}(\epsilon, l) = \begin{cases} -B(k,l)(\eta_1\eta_3 + \eta_2\eta_4), & \epsilon > 0 \\ -\frac{1}{2}A(\nu, l)(D^2(\eta_1 + i\eta_2)(\eta_3 + i\eta_4)\exp[i\pi(l-\frac{1}{2})] \\ \qquad + D^{-2}\mathrm{Re}\{(\eta_1 - i\eta_2)\exp[-\frac{1}{2}i\pi(l+\frac{1}{2})]\}\mathrm{Re}\{(\eta_3 - i\eta_4)\exp[-\frac{1}{2}i\pi(l+\frac{1}{2})]\}), & \epsilon < 0. \end{cases} \qquad (2.17)$$

These expressions complement Table I of GFS in specifying the QDT parameters for arbitrary long-range fields. These QDT parameters are graphed in Figs. 1–4. The range of the parameter kf (or f/ν) covered here is sufficient, e.g., for the analyses of low-energy (0 ~ 10 eV) elastic scattering of an electron by noble gases or for studying many of the electron-alkali atom compounds near the first fine-structure threshold energies. Note that the Mathieu equation involves the parameters $k(1/\nu)$ and f only in the product form $kf(f/\nu)$.

In the small $kf(f/\nu)$ limit, OSR's series expression[5] [Eqs. (3.6) and (3.10)] for m and τ yields the QDT parameters to leading order in $kf(f/\nu)$ as

$$2D^2A^{-1}(\nu, l) = \begin{cases} f/\nu, & l = 0 \\ \dfrac{\pi^2[(2l+1)!!]^4}{(2l+3)^2(2l-1)^2(2l+1)^4}(f/\nu)^{3-2l}, & l \geqslant 1 \end{cases}$$

$$B^{-1}(k, l) = \begin{cases} kf, & l = 0 \\ \dfrac{\pi^2[(2l+1)!!]^4}{(2l+3)^2(2l-1)^2(2l+1)^4}(kf)^{3-2l}, & l \geqslant 1 \end{cases} \qquad (2.18)$$

$$\eta(k, l) = \begin{cases} \pi/2 - \pi kf/3, & l = 0 \\ -5kf/3\pi - \pi/2, & l = 1 \\ \dfrac{\pi(kf)^2}{(2l+3)(2l+1)(2l-1)} - \frac{1}{2}\pi l, & l \geqslant 2 \end{cases}$$

$$\mathcal{G}(\epsilon, l) = \begin{cases} -\pi(1-kf)/3, & l = 0, \quad \epsilon > 0 \\ \nu/f, & l = 0, \quad \epsilon < 0 \\ \dfrac{(2l+3)(2l+1)(2l-1)}{\pi f^2\epsilon}, & l \geqslant 1 \quad \epsilon \gtrless 0 \end{cases}$$

and $D^2 \simeq |(l+1)\pi - \beta|$ approaches zero at least as rapidly as $(f/\nu)^2$ for $l = 0$ and much more rapidly for $l \geqslant 1$. The energy dependence of A and D near threshold is given here only for the product D^2/A, as they appear only in this combination in our applications. The behavior of $\mathcal{G}(\epsilon, l)$ near threshold is independent of the choice of $\beta(\nu, l)$.

Delves[16] has shown that the threshold behavior of the phase shift in the presence of a long-range field $V_n = -f_n^2/2r^n$, is

$$\delta_l \propto \begin{cases} \epsilon^{l+1/2} & (n \geqslant 2l+3) \\ \epsilon^{n/2-1} & (n \leqslant 2l+3) \end{cases} \quad (\epsilon > 0). \qquad (2.19)$$

One can show that this agrees with our present results.

General behaviors of the QDT parameters we have obtained can be understood by a WKB-type consideration. Our choice of $\eta(k, l)$ and $\beta(\nu, l)$ corresponds to setting the phase integral at small r,

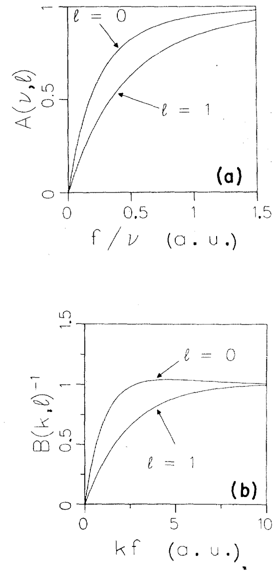

FIG. 1. Amplitude parameters versus reduced energy parameter for $l=0$ and 1: (a) $A(\nu,l)$ below threshold; (b) reciprocal of amplitude $B^{-1}(k,l)$ above threshold. Note convergence to unity away from threshold, more rapidly for $l=0$.

$$\delta_l^{\mathrm{WKB}}(r) = -\lim_{r_0\to 0}\left[\int_{r_0}^{r}\left(\epsilon-\frac{(l+\frac{1}{2})^2}{r^2}+\frac{f^2}{r^4}\right)^{1/2}dr-f/r_0\right]$$

$$+\tfrac{1}{2}l\pi \xrightarrow[|r|\ll 1]{} (f/r-l\pi/2)+l\pi\,, \qquad (2.20)$$

for both $\epsilon > 0$ and $\epsilon < 0$. The rapid variation of the amplitudes of B and $\mathcal{G}$ in the region of small kf arises from the penetration of the effective centrifugal barier $(l+\frac{1}{2})^2/r^2$. At large kf instead, B approaches unity and $\mathcal{G}$ vanishes.

Analogous comments apply to A and $\mathcal{G}$ below threshold. Note, however, the convergence of $\mathcal{G}$ to $-\pi/3$ for $l=0$ as $\epsilon\to 0^+$ while it diverges as $\epsilon\to 0^-$. For higher angular momenta $\mathcal{G}$ diverges as $1/\epsilon$ at $\epsilon=0$. The phase shifts β and η both decrease far away from threshold as expected. [Figure 3(b) shows the noncentrifugal part of the phase shift $\eta(k,l)+\frac{1}{2}l\pi$.] The scaling parameter D steadily rises as f/ν increases. Some useful values of the quantum-defect parameters are given in Tables I and II for $l=0$.

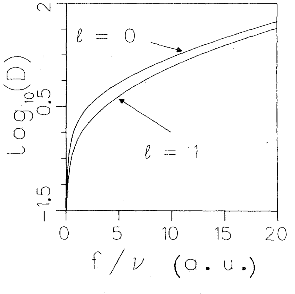

FIG. 2. Amplitude scaling parameter $D(\nu,l)(\epsilon<0)$ versus energy parameter f/ν.

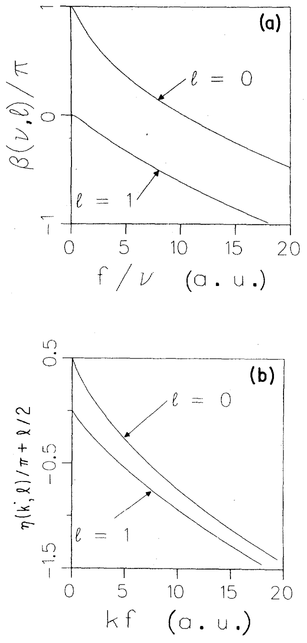

FIG. 3. Phase shifts versus energy for $l=0$ and 1. (a) Negative energy phase $\beta(\nu,l)$. (b) Positive energy, noncentrifugal part of phase $\eta(k,l)+\frac{1}{2}l\pi$.

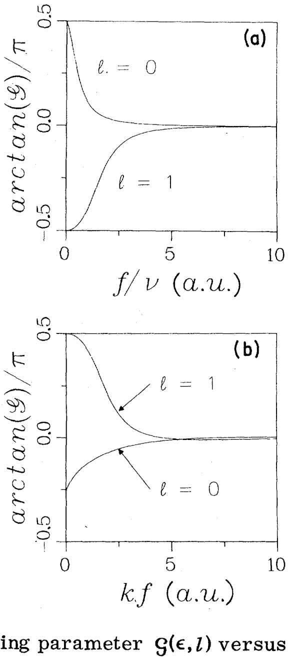

FIG. 4. Mixing parameter $\mathcal{G}(\epsilon,l)$ versus energy. (a) Negative energy; (b) positive energy. Arctan ($\mathcal{G}$) is shown because $\mathcal{G}$ diverges near threshold except for $l=0$ and positive energy.

TABLE I. Values of quantum-defect parameters for $l=0$. Negative energies $5\times10^{-2}\leqslant f/\nu\leqslant 5$.

f/ν ($10^{(n)}$)	A ($10^{(n)}$)	β/π ($10^{(n)}$)	$\mathcal{G}$ ($10^{(n)}$)	D ($10^{(n)}$)
5 (−2)	1.876 (−1)	1 − 1.503 (−3)	1.884 (1)	7.237 (−2)
1 (−1)	3.355 (−1)	1 − 5.438 (−3)	8.829 (0)	1.447 (−1)
2 (−1)	5.438 (−1)	1 − 1.804 (−2)	3.884 (0)	2.896 (−1)
3 (−1)	6.761 (−1)	1 − 3.428 (−2)	2.299 (0)	4.346 (−1)
4 (−1)	7.632 (−1)	1 − 5.233 (−2)	1.546 (0)	5.799 (−1)
5 (−1)	8.227 (−1)	1 − 7.116 (−2)	1.119 (0)	7.256 (−1)
6 (−1)	8.645 (−1)	1 − 9.024 (−2)	8.508 (−1)	8.718 (−1)
7 (−1)	8.948 (−1)	8.907 (−1)	6.695 (−1)	1.019 (0)
8 (−1)	9.171 (−1)	8.720 (−1)	5.407 (−1)	1.166 (0)
9 (−1)	9.339 (−1)	8.536 (−1)	4.456 (−1)	1.314 (0)
1 (0)	9.468 (−1)	8.356 (−1)	3.734 (−1)	1.463 (0)
2 (0)	9.914 (−1)	6.787 (−1)	1.041 (−1)	3.022 (0)
3 (0)	9.981 (−1)	5.548 (−1)	4.369 (−2)	4.766 (0)
4 (0)	9.995 (−1)	4.517 (−1)	2.182 (−2)	6.781 (0)
5 (0)	9.999 (−1)	3.623 (−1)	1.202 (−2)	9.143 (0)

III. APPLICATION TO K⁻ PHOTODETACHMENT

We have seen how Norcross and Taylor[4(a)] calculated a reaction matrix and a dipole matrix for the photodetached P states of K⁻ and found them to be strongly energy dependent in a narrow range near the $4p$ detachment threshold. In this section we shall show how equivalent results can be expressed in terms of a reaction matrix and a dipole matrix, both energy independent in the same range, provided the polarizability of K in its $4p$ state is taken into account by using the wave functions described in Sec. II.

TABLE II. Positive energies $5\times10^{-2}\leqslant kf\leqslant 5$.

kf	B	η/π	$\mathcal{G}$
5 (−2)	2.014 (1)	4.840 (−1)	−9.616 (−1)
1 (−1)	1.021 (1)	4.691 (−1)	−8.959 (−1)
2 (−1)	5.285 (0)	4.416 (−1)	−7.950 (−1)
3 (−1)	3.668 (0)	4.163 (−1)	−7.178 (−1)
4 (−1)	2.870 (0)	3.927 (−1)	−6.552 (−1)
5 (−1)	2.397 (0)	3.704 (−1)	−6.026 (−1)
6 (−1)	2.086 (0)	3.491 (−1)	−5.573 (−1)
7 (−1)	1.867 (0)	3.287 (−1)	−5.175 (−1)
8 (−1)	1.705 (0)	3.091 (−1)	−4.822 (−1)
9 (−1)	1.581 (0)	2.901 (−1)	−4.505 (−1)
1 (0)	1.484 (0)	2.717 (−1)	−4.218 (−1)
2 (0)	1.083 (0)	1.094 (−1)	−2.230 (−1)
3 (0)	9.880 (−1)	−2.916 (−2)	−1.307 (−1)
4 (0)	9.629 (−1)	−1.536 (−1)	−7.087 (−2)
5 (0)	9.608 (−1)	−2.680 (−1)	−3.499 (−2)

Stationary-state wave functions of the continuous spectrum of a multichannel system such as K⁻ can be expressed for large r in the form

$$\psi_i = r^{-1}\mathfrak{a}\sum_j \phi_j[f_j(r)\delta_{ij} - K_{ij}g_j(r)]\,. \tag{3.1}$$

Here ϕ_i indicates a wave function for the ith channel of K⁻ including its dependence on all variables except the radial distance of the detached electron, (f_i, g_i) indicate a base pair of radial functions for the detached electron, K_{ij} is a reaction matrix, and the symbol $\mathfrak{a}$ indicates antisymmetrization of r with the coordinates of other electrons. In the most familiar formulation, the $f_i(r)$ functions are Riccati-Bessel functions normalized per unit energy and the g_i are of the corresponding Neumann kind. Norcross and Taylor instead renormalized these functions to a form energy independent at $r\sim0$ in order to minimize the energy dependence of the reaction matrix. Removal of the residual energy dependence will be achieved here by replacing the pair (f_i, g_i), for the channel with the K residue in its $4p$ state, with a base pair for the polarization field as defined in Eq. (2.7).

The alternative pair will be distinguished by adding a "zero-field" index "z" to the Norcross-Taylor pair (f_i^z, g_i^z), and a "polarization-field" index "p" to the pair (2.7). We shall instead omit, for brevity, the index "o" that would pertain to all these functions according to the notations of Sec. II and of GFS. Similarly, we shall label the $\underline{K}$ matrix with superscripts z or p, omitting the label o. The desired relationship between $\underline{K}^p$ and $\underline{K}^z$ is to be obtained by comparing the expansions (3.1) of ψ_i^p and ψ_i^z, taking into account the relationship between the (f_i^p, g_i^p) and the (f_i^z, g_i^z) pairs.

In the energy range of interest, near the $4p$ threshold, there are only two open P channels of K⁻, namely $4s\epsilon p$ and $4p\epsilon s$. Triplet and singlet states of K⁻ will be treated separately, as was done by Norcross and Taylor,[4(a)] but both of them must be studied since they must be combined in the eventual consideration of spin-orbit coupling. The calculation of Ref. 4(a) included the additional closed P channels $4p\epsilon d$, $5s\epsilon p$, and $3d\epsilon p$ because they interact with the open channels appreciably. Here we need to consider these channels explicitly only for the limited purpose of evaluating the polarizability of the $4p$ state of K as described below. The short-range contributions of the coupling with closed channels are energy independent on the scale of interest, and hence will be taken into account implicitly in the process of fitting the two-channel matrix $\underline{K}^p$ semiempirically. For the same reason it will be sufficient for us to carry out the transformation from $\underline{K}^z$ to $\underline{K}^p$, replacing explicitly the z pair with the p pair for the $4p\epsilon s$ *channel only*. The polarizability of K in its $4s$ state will be embodied in the fitted $\underline{K}^p$ matrix. (The $4s$ polarizability should lead to no noticeable variation with energy in the range of interest near the $4p$ threshold.)

The connection between the p and z pairs is represented by a matrix $\underline{\Gamma}$ as in Eq. (3.1) of Ref. 6,

$$f^p=\Gamma_{ff}f^z+\Gamma_{fg}g^z\,,$$
$$g^p=\Gamma_{gf}f^z+\Gamma_{gg}g^z\,. \tag{3.2}$$

This matrix is calculated by representing both the p and the z pair in terms of a third base pair adapted to $r\to\infty$ and hence independent of polarizability, namely, $\{\cos kr,\ \sin kr\}$ for $\epsilon>0$ and $\{\exp(r/\nu),\ \exp(-r/\nu)\}$ for $\epsilon<0$, with $\epsilon=k^2=-1/\nu^2$ Rydberg units. The transformation to this base is done again in two steps, by going over first to an energy-normalized pair and then to the $r\to\infty$ pair. The transformation matrix pertaining to the p pair is given by the reciprocal of the matrix in Eq. (2.14) for the first step and is obtained from Eqs. (2.10) and (2.11) for the second step. The corresponding matrices for the z pair are obtained from Table I (B) and I (C) of GFS, respectively. Combining these 4 factors, we find

$$\underline{\Gamma}=\begin{bmatrix} B_p^{1/2} & 0 \\ B_p^{-1/2}\mathcal{G}_p & B_p^{-1/2}\end{bmatrix}^{-1}\begin{bmatrix}\cos\eta_p & \sin\eta_p \\ -\sin\eta_p & \cos\eta_p\end{bmatrix}^{-1}$$
$$\times\begin{bmatrix}\cos\eta_z & \sin\eta_z \\ -\sin\eta_z & \cos\eta_z\end{bmatrix}\begin{bmatrix} B_z^{1/2} & 0 \\ B_z^{-1/2}\mathcal{G}_z & B_z^{-1/2}\end{bmatrix}, \tag{3.3a}$$

at positive energies $\epsilon>0$ and

$$\underline{\Gamma}=\begin{bmatrix} A_p^{1/2} & 0 \\ A_p^{-1/2}\mathcal{G}_p & A_p^{-1/2}\end{bmatrix}^{-1}\begin{bmatrix}\cos\beta_p D_p^{-1} & \sin\beta_p D_p^{-1} \\ -\sin\beta_p D_p & \cos\beta_p D_p\end{bmatrix}^{-1}$$
$$\times\begin{bmatrix}\cos\beta_z D_z^{-1} & \sin\beta_z D_z^{-1} \\ -\sin\beta_z D_z & \cos\beta_z D_z\end{bmatrix}\begin{bmatrix} A_z^{1/2} & 0 \\ A_z^{-1/2}\mathcal{G}_z & A_z^{-1/2}\end{bmatrix}, \tag{3.3b}$$

at negative energies $\epsilon<0$. The QDT parameters for the zero field are tabulated in GFS (Table I).

The parameters A_p, B_p, $\mathcal{G}_p$, β_p, η_p, and D_p in these expressions are functions of the polarizability α described by (2.17) and earlier equations of Sec. II. The value of α itself has been calculated by the familiar-looking formula

$$\alpha=2\sum_n\frac{|D_{n,4p}|^2}{E_n-E_{4p}}\,, \tag{3.4}$$

where n indicates one of the even-parity levels of K, i.e., $4s$, $3d$, $5s$, and implies summation over magnetic quantum numbers m_l associated with n. The derivation and the evaluation of this formula in the present context require some discussion which is given in the Appendix.

The final step of obtaining the $\underline{K}^z$ matrix from $\underline{K}^p$ utilizes the explicit expression of the wave functions (3.1) for our system with two open channels. We label 1 the channel ($4s\epsilon p$) and (f_1,g_1) its single set of base functions. We label 2 the channel ($4p\epsilon s$) and (f_2^p,g_2^p) and (f_2^z,g_2^z) its two alternative sets of base functions. The explicit form of the base wave functions (3.1) of the p type is (omitting r^{-1} and $\mathfrak{A}$)

$$(\phi_1f_1-K_{11}^p\phi_1g_1-K_{12}^p\phi_2g_2\,,\ \phi_2f_2^p$$
$$-K_{21}^p\phi_1f_1-K_{22}^p\phi_2f_2^p).$$

Each of these functions must be expressible as a superposition of the corresponding pair of wave functions of the z type. Thus, we write

$$\begin{aligned}\phi_1f_1-K_{11}^p\phi_1g_1-K_{12}^p\phi_2g_2^p&\\ &=L(\phi_1f_1-K_{11}^z\phi_1g_1-K_{12}^z\phi_2g_2^z)\\ &\quad+M(\phi_2f_2^z-K_{21}^z\phi_1g_1-K_{22}^z\phi_2g_2^z)\,,\\ \phi_2f_2^p-K_{21}^p\phi_1g_1-K_{22}^p\phi_2g_2^p&\\ &=P(\phi_1f_1-K_{11}^z\phi_1g_1-K_{12}^z\phi_2g_2^z)\\ &\quad+Q(\phi_2f_2^z-K_{21}^z\phi_1g_1-K_{22}^z\phi_2g_2^z)\,.\end{aligned} \tag{3.5}$$

Substituting the expressions (3.2) on the left-hand side, we obtain two linear relations involving the four independent functions ϕ_1f_1, ϕ_1g_1, $\phi_2f_2^z$, and $\phi_2g_2^z$. The coefficients of each of these functions must be equal on the two sides of each Eq. (3.5); this yields eight inhomogeneous equations in L, M, P, Q, K_{11}^z, K_{12}^z, K_{21}^z, and K_{22}^z. This system can be solved directly or more generally by the matrix algebra reformulation given in the preceding paper[6]:

$$\begin{bmatrix} L & M \\ P & Q\end{bmatrix}=\begin{bmatrix} 1 & M \\ 0 & Q\end{bmatrix}=\begin{bmatrix} 1 & -K_{12}^p\Gamma_{gf} \\ 0 & \Gamma_{ff}-K_{22}^p\Gamma_{gf}\end{bmatrix} \tag{3.6a}$$

and

$$\underline{K}^z=\frac{1}{Q}\begin{bmatrix} K_{11}^pQ+K_{21}^pK_{12}^p\Gamma_{gf} & K_{12}^p \\ K_{21}^p & K_{22}^p\Gamma_{gg}-\Gamma_{fg}\end{bmatrix}. \tag{3.6b}$$

The matrix (3.6a) will prove useful later in transforming the dipole matrix from the zero-field representation to the polarization-field representation and vice versa.

The relationship thus established between the matrices $\underline{K}^z$ and $\underline{K}^p$, whose coefficients depend on the energy through the elements of the matrix $\underline{\Gamma}$, was utilized in the following way. At the energy

$E_{\rm fit} = 5 \times 10^{-4}$ Ry above the $4p$ threshold, the matrix K^z was given the values calculated by Norcross and Taylor,[4(a)] and the matrix $\underline{K}^p$ was calculated from it:

$$\underline{K}^p = \begin{cases} \begin{pmatrix} 19.31 & -5.28 \\ -5.28 & 0.376 \end{pmatrix} \text{ for } S=0 \\ \begin{pmatrix} 90.11 & 0.652 \\ 0.652 & -0.130 \end{pmatrix} \text{ for } S=1\,. \end{cases}$$

At the other energies shown in Fig. 1, $\underline{K}^p$ was given the same values as at $E_{\rm fit}$; $\underline{K}^z$ was then calculated and compared with the Norcross-Taylor matrix in terms of the alternative parameters, namely, the mixing angle Θ and two eigenphase shifts μ_1 and μ_2 which are related to the matrix $\underline{K}^z$ by the following expressions:

$$\left.\begin{array}{l}\pi\mu_1 \\ \pi\mu_2\end{array}\right\} = \tan^{-1}\{(K^z_{11}+K^z_{22})/2 \pm[(K^z_{11}-K^z_{22})^2/4+K^z_{12}K^z_{21}]^{1/2}\},$$

$$\Theta = \tan^{-1}[2K^z_{12}/(K^z_{22}-K^z_{11})]/2\,, \tag{3.7}$$

$$\underline{U} = \begin{pmatrix} \cos\Theta & \sin\Theta \\ -\sin\Theta & \cos\Theta \end{pmatrix},$$

where $\underline{U}$ diagonalizes the K matrix as in Eq. (2.6) of Ref. 6.

Figure 5(a) shows a weak asymmetric cusp for $S=0$ near threshold, indicating the opening of the channel $4p\epsilon s$. Figure 5(b) shows a sharply avoided crossing for $S=1$ at $\epsilon \cong 2.7$ meV. The origin of the cusp is traced to the nonanalyticity of $\mathcal{G}$ through the substitution of small $kf(f/\nu)$ expansions. We have

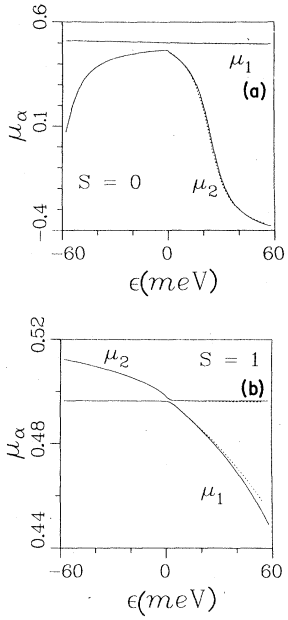

FIG. 5. Comparison of the analytically fitted (——) and numerical [---- Ref. 4(a)] eigenphases. (a) $S=0$; (b) $S=1$. Note cusp at threshold for $S=0$ and expanded scale of μ_α for $S=1$.

$$\underline{\Gamma} = \begin{cases} \begin{bmatrix} \pi f^{3/2}\epsilon/3 & -f^{1/2} \\ f^{-1/2} & \pi f^{3/2}\epsilon^{1/2}/3 \end{bmatrix}, & \epsilon \gtrsim 0 \\ \begin{bmatrix} \pi f^{3/2}\epsilon/3 & -f^{1/2} \\ f^{-1/2} & O(\epsilon^2) \end{bmatrix}, & \epsilon \lesssim 0 \end{cases} \tag{3.8}$$

and consequently,

$$K^z_{22} = \begin{cases} (K^p_{22}\pi f^{3/2}/3 + f^{1/2})/(\pi f^{3/2}\epsilon/3 - K^p_{22}f^{-1/2}) & \epsilon \gtrsim 0 \\ -f/K^p_{22} & \epsilon \lesssim 0\,. \end{cases} \tag{3.9}$$

Thus, $\lim_{\epsilon\to 0+} dK^z_{22}/d\epsilon = \infty$ while $\lim_{\epsilon\to 0-} dK^z_{22}/d\epsilon = 0$. A cusp is missing in Fig. 5(b) for $S=1$ due to the occurrence of the avoided crossing near threshold. The mixing of the singlet states is large but the triplet states remain almost decoupled. Notice the step in Θ for $S=1$ near threshold where the eigenphases have the avoided crossing.

Analogously, we reproduced the energy of the dipole matrix of Norcross and Taylor from an energy-independent matrix utilizing the transformation (3.6a). For example, the dipole matrix element in the polarization representation evaluated between the ground-state wave function $\psi_{\rm ground}$ of the electron-neutral atom compound and the first dissociation channel wave function ψ^p_1, is given by

$$D^p_1 = (\psi_{\rm ground}|d|\psi^p_1)\,, \tag{3.10}$$

where d is the dipole operator and ψ^p_1 is that solution which asymptotically approaches $\phi_1 f_1 - K^p_{11}\phi_1 g_1 - K^p_{12}\phi_2 g^p_2$. The above can be expressed as a linear combination of the dipole matrix elements in the zero-field representation by substituting expressions (3.5) into Eq. (3.10). We then have

$$D^p_1 = (\phi_{\rm ground}|d|L\psi^z_1 + M\psi^z_2) = LD^z_1 + MD^z_2\,, \tag{3.11a}$$

where ψ^z_1 and ψ^z_2 are the corresponding zero-field solutions which asymptotically approach $\phi_1 f_1 - K^z_{11}\phi_1 g_1 - K^z_{12}\phi_2 g^z_2$ and $\phi_2 f^z_2 - K^z_{21}\phi_1 g_1 - K^z_{22}\phi_2 g^z_2$, respectively. Similarly, we express D^p_2 in terms

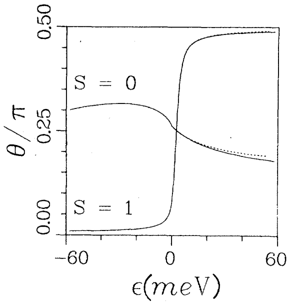

FIG. 6. Comparison of analytical (——) and numerical [----, Ref. 4(a)] values for the angle Θ representing the mixing of ($4s\epsilon p$) and ($4p\epsilon s$) channels for $S=0$, 1. The sharp step in the $S=1$ curve derives from the avoided crossing of phase shifts in Fig. 1(b). Note the small cusp for $S=0$ at threshold.

of D^g_1 and D^g_2 as

$$D^p_2=PD^g_1+QD^g_2 . \tag{3.11b}$$

Thus,

$$\begin{pmatrix} D^p_1 \\ D^p_2 \end{pmatrix} = \begin{pmatrix} 1 & M \\ 0 & Q \end{pmatrix} \begin{pmatrix} D^g_1 \\ D^g_2 \end{pmatrix} , \tag{3.12a}$$

or equivalently,

$$\begin{pmatrix} D^g_1 \\ D^g_2 \end{pmatrix} = \frac{1}{Q} \begin{pmatrix} Q & -M \\ 0 & 1 \end{pmatrix} \begin{pmatrix} D^p_1 \\ D^p_2 \end{pmatrix} . \tag{3.12b}$$

The dipole matrix above is related to the dipole matrix in the eigenchannel representation given in Sec. II of the preceding paper[6] by

$$D^p_\alpha = \sum_i D^p_i \cos\pi\mu_i U_{i\alpha} . \tag{3.13}$$

The above results (3.12) establish explicitly the connection between (D^g_1, D^g_2) and (D^p_1, D^p_2) in terms of the base transformation matrix (3.2). The energy dependence is thus absorbed into $\underline{\Gamma}$ through M, Q. This point is illustrated in Fig. 7 which was generated by Eq. (3.12b) using an energy-independent dipole matrix $\underline{D}^p$ fitted to the Norcross-Taylor matrix[4(a)] at one energy $E_{\text{fit}}=5\times10^{-4}$ Ry ($D^p_1=-97.15$, $D^p_2=23.84$). Both D^g_1 and D^g_2 grow in comparable magnitudes away from threshold, reflecting the large mixing of the $4p\epsilon s$ and $4s\epsilon p$ states. The total and partial cross sections obtained using the fitted values of μ_1, μ_2, and Θ, and of the dipole matrix appear identical to the Norcross-Taylor cross sections,[4(a)] though we do not show them here.

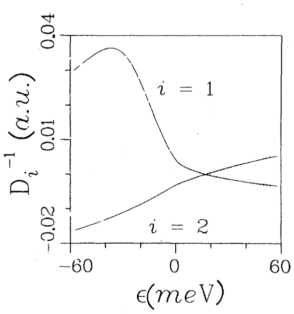

FIG. 7. Comparison of the analytically fitted (——) and numerical [----, Ref. 4(a)] dipole matrix elements. Reciprocals are plotted to avoid a divergence of unnormalized data.

The present results have shown that the energy dependence of K^g_{ij} and D^g_i calculated by Norcross and Taylor results from the polarizability of potassium. It is not obvious, however, that the energy dependence arises only from a phase shift, as found by Norcross and Taylor, and as implied by Eq. (1.1). We have determined by direct calculation that the energy dependence of *K^g_{ij} implied by $\delta=\eta_p$ in Eq.* (1.1) *alone*, does *qualitatively* reproduce that shown in Figs. 5–7. Still, to reproduce the energy dependence quantitatively, we have found it necessary to use the full transformation given in Eq. (3.3b).

ACKNOWLEDGMENTS

We are indebted to Professor U. Fano for extensive discussions and suggestions, and also for his assistance with the manuscript. Thanks are also due to Dr. D. W. Norcross and Dr. K. T. Taylor for communicating their results prior to publication. Suggestions by Dr. J. Siegel greatly simplified the graphical work. This work was supported by the U. S. Department of Energy, Office of Basic Energy Sciences. One of us (C.H.G.) was partially supported by an IBM Graduate Fellowship.

APPENDIX: DERIVATION OF THE POLARIZATION POTENTIAL FROM THE CLOSE-COUPLING EQUATIONS

It was shown long ago[11] that the close-coupling equations for an electron in the field of an atom reduce as $r\to\infty$ to a set of uncoupled radial Schrödinger equations with a polarization potential $-\alpha^{st}/2r^4$. Castillejo *et al.*[11] noted that α^{st} is the static polarizability of the atomic state associated with a channel, provided this state has zero orbital angular momentum. Alternative derivations have also been given in the literature[9,17,18,10] which confirm this result and extend it by deriving correction terms that vary as r^{-6}. In the context of the present paper it seemed worthwhile to present a comprehensive derivation of these results, spelling out the role of the adiabatic approximation which had not always been stated explicitly, and the dependence of the polarizability α_μ^{st} for the μth channel on this channel's parameters. In so doing, we have found two features:

(i) the actual coefficient of the r^{-4} potential depends on the orbital angular momenta of the atom l_1 and of the outermost electron l_2, and in particular it differs from the static polarizability α^{st} when both $l_1 \neq 0$ and $l_2 \neq 0$.

(ii) the r^{-6} term in the interaction has three contributions; one is adiabatic and results from the centrifugal potential of the outer electron, and the others are nonadiabatic and result from the actual *radial* motion of the outer electron.[19] The net result of item (ii) reduces to the well-known correction term $6\beta/2r^6$ in special circumstances.

In the close-coupling equations for the radial wave function $M_j(r)$ of the detached photoelectron in the jth dissociation channel, the potential is local and off-diagonal at large $r \geq r_0$,

$$\left[-\tfrac{1}{2}\frac{d^2}{dr^2}+\tfrac{1}{2}\,\frac{l_j(l_j+1)}{r^2}-\epsilon_j\right]M_j(r)+\sum_i V_{ji}(r)M_i(r)=0\,. \tag{A1}$$

Here $\epsilon_j \equiv E - E_j$ is the energy relative to the atomic state of energy E_j associated with the jth channel. This local form of the equations of motion does not hold at smaller r where nonlocal exchange terms are important. The real symmetric potential matrix is defined by

$$V_{ji}(r) \equiv (\phi_j(\omega)\,|V|\,\phi_i(\omega))\,, \tag{A2}$$

where V is the electrostatic potential between the N core electrons and the detached electron, and $\phi_i(\omega)$ is a bound-core wave function LS coupled to the orbital and spin functions of the outermost electron with specified values of L and S. The matrix element in (A2) implies integration over all degrees of freedom except the radial coordinate r.

We proceed to diagonalize Eq. (A1) adiabatically at fixed r, thereby reducing the long-range coupling from r^{-2} to r^{-3}.[20] Mathematically this is accomplished by transforming Eq. (A1) with an orthogonal matrix $\underline{W}(r)$:

$$\begin{aligned}[E_\mu+u_\mu(r)]\delta_{\mu\mu'} = \sum_{ij} W_{\mu i}(r) \\ \times[l_i(l_i+1)/2r^2\delta_{ij}+E_i\delta_{ij}+V_{ij}(r)] \\ \times[W^T(r)]_{j\mu'}\,.\end{aligned} \tag{A3}$$

Here the adiabatic channels are labeled by Greek letters. The potential energy $u_\mu(r)$ vanishes when $r\to\infty$, and $W_{\mu i}(r)$ reduces to $\delta_{\mu i}$ in this limit. (This presumes that no atomic states of opposite parity are accidentally degenerate as in hydrogen.) Accordingly, the adiabatic μ channels can be set in one-to-one correspondence with the i channels to which they converge as $r\to\infty$. In the following, we use both Greek and Roman indices with the understanding that they coincide at large r (e.g., $\mu=1$ coincides with $i=1$ at $r=\infty$).

This transformation of Eq. (A1) gives rigorously[21,22]

$$\left[-\tfrac{1}{2}\left(\underline{1}\frac{d}{dr}+\underline{P}(r)\right)^2-[\underline{\epsilon}-\underline{u}(r)]\right]\vec{\mathrm{F}}(r)=0\,, \tag{A4}$$

where

$$\vec{\mathrm{F}}(r)=\underline{W}(r)\vec{\mathrm{M}}(r)$$

and

$$\underline{P}(r)=\underline{W}(r)\frac{d}{dr}\underline{W}^T(r)\,.$$

The diagonal matrix $\underline{\epsilon}$ represents the energy relative to threshold in each channel $\epsilon_\mu = E - E_\mu$. The antisymmetric matrix $\underline{P}(r)$ now contains all of the residual interchannel coupling.

To lowest significant order in r^{-1}, we need to retain only the dipole couplings in (A2), given by

$$\begin{aligned}V_{ji}(r) &= \Big(\phi_j(\omega)\,|\hat{r}\cdot\sum_k \vec{\mathrm{r}}_k\,|\,\phi_i(\omega)\Big)/r^2 \\ &\equiv \overline{V}_{ji}/r^2\,.\end{aligned} \tag{A5}$$

Here $\vec{\mathrm{r}}_k$ is the position vector of the kth atomic electron. At sufficiently large r the $V_{ji}(r)$ are small compared to the atomic energy level separation $E_i - E_j$, so the diagonalization (A3) can be performed perturbatively.[23] We find

$$\begin{aligned}u_\mu(r) &= l_\mu(l_\mu+1)/2r^2-\alpha_\mu/2r^4+\beta_\mu^a/2r^6+O(r^{-8})\,,\\ W_{\mu i}(r) &= \left(\delta_{\mu i}+\frac{1}{r^2}\frac{\overline{V}_{\mu i}}{E_\mu-E_i+[l_\mu(l_\mu+1)-l_i(l_i+1)]/2r^2}+O(r^{-4})\right)N_\mu(r)\,,\\ P_{\mu\nu}(r) &= \begin{cases}-\dfrac{1}{r^3}\dfrac{2\overline{V}_{\mu\nu}}{E_\mu-E_\nu}+O(r^{-5})\,, & \mu\neq\nu\\ 0\,, & \mu=\nu\end{cases}\end{aligned} \tag{A6}$$

where $N_\mu(r)=1+O(r^{-4})$ is a normalization factor.

Explicit expressions for α_μ and β_μ^a will be given below in Eq. (A10). First, however, we note that the transformation $W_{\mu i}(r)$ has reduced the off-diagonal coupling[20] at large r from r^{-2} in Eq. (A1) to r^{-3} in Eq. (A4). To a good approximation then, $\underline{P}(r)$ can be neglected entirely in the outer region and $\beta_\mu^a/2r^6$ (and all higher terms) can be ignored in $u_\mu(r)$. These are the only approximations used in the treatment of Sec. III, and Figs. 5–7 indicate that the errors involved are negligible. The validity of ignoring β_μ^a and higher-order terms in $u_\mu(r)$ is investigated quantitatively in Fig. 8, which compares the exactly diagonalized potential $u_\mu(r)$ (for the $4p\epsilon s$ channel of K$^-$) with the polarizability potential alone. The radius of the inner region is roughly $r_0\approx 30$ a.u. for this channel. At that radius we estimate the exchange energy to be 2% of the polarization energy. The relative error incurred in Fig. 8 by using only the first two terms in $u_\mu(r)$ is then roughly 10% at $r=r_0$, and is decaying rapidly as r^{-2}.

Next we turn to items (i) and (ii) above, in succession. First, the dependence of the effective polarizability α_μ on the angular momentum of the outer electron is now clear; α_μ depends through Eq. (A5) on $\overline{V}_{ji}$, given for a two-electron system[24,25]

$$
\begin{aligned}
\overline{V}_{ji} &= ((n_j l_{1j}\epsilon_j l_{2j})LM\,|r_1\cos\Theta_{12}|\,(n_i l_{1i}\epsilon_i l_{2i})LM)\\
&=\frac{1}{\sqrt{2L+1}}((l_{1j}l_{2j})L\|\cos\Theta_{12}\|(l_{1i}l_{2i})L)R^{n_j l_{1j}}_{n_i l_{1i}}\\
&=(-1)^{L+l_{2j}+l_{1j}}\begin{Bmatrix} l_{1j} & l_{2j} & L\\ l_{2i} & l_{1i} & 1\end{Bmatrix}(l_{1j}\|\cos\Theta_1\|l_{1i})\\
&\quad\times(l_{2j}\|\cos\Theta_2\|l_{2i})R^{n_j l_{1j}}_{n_i l_{1i}}\,. \qquad \text{(A7)}
\end{aligned}
$$

Here $R^{n_j l_j}_{n_i l_i}$ is the radial matrix element and (n,l_1) are the principal and orbital quantum numbers of the atomic valence electron, respectively. Subscripts 1 and 2 refer, in the following, to the valence and detached electrons, respectively. The reduced matrix element is evaluated in Eq. (3.14) of Ref. 25 and depends explicitly on (l_2l_2') and on L. In the usual expression for the static polarizability of the state (nl_1), this matrix element is replaced by its single factor $(l_1\|\cos\Theta_1\|l_1')$ which obviously depends neither on (l_2l_2') nor on L. In special cases (e.g., when $l_1=0$), the effective polarizability α_μ in Eq. (A10) reduces to the static polarizability by virtue of the properties of 3-j and 6-j symbols.[25] An example of this difference among polarizabilities is provided by our estimates using Bates-Damgaard radial integrals[26] for K$^-$:

$$\alpha_{4p}^{\rm st}=\alpha_{4p\epsilon s}=600\ \text{a.u.}\,,$$

$$\alpha_{4p\epsilon d}=690\ \text{a.u.}$$

Second, we discuss item (ii) regarding the coefficient of the r^{-6} long-range potential, without considering the quadrupole interaction in (A2). The "post-adiabatic" theory of Klar and Fano[21,22] derives the nonadiabatic effect of $\underline{P}(r)$ on the potential energy

$$
\begin{aligned}
u_\mu^{\rm eff}(r)&=u_\mu(r)-\tfrac{1}{2}(\underline{P}^2)_{\mu\mu}\\
&\quad+2(E-E_\mu-u_\mu)\sum_\nu\frac{|P_{\mu\nu}|^2}{E_\mu+u_\mu-E_\nu-u_\nu}+\cdots\,, \qquad \text{(A8)}
\end{aligned}
$$

for $\frac{1}{2}|P_{\mu\nu}(r)|^2\ll|E_\mu(r)-E_\nu(r)|$. Using the perturbation expansion for $u_\mu(r)$ and $P_{\mu\nu}(r)$ in (A6), we obtain finally

$$
\begin{aligned}
u_\mu^{\rm eff}(r)&=\frac{l_\mu(l_\mu+1)}{2r^2}-\frac{\alpha_\mu}{2r^4}\\
&\quad+\frac{(\beta_\mu^a+\beta_\mu^{na})-2(E-E_\mu)\gamma_\mu}{2r^6}+O(r^{-8})\,, \qquad \text{(A9)}
\end{aligned}
$$

where

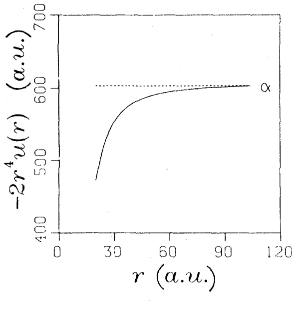

FIG. 8. Effective polarizability $\alpha(r)$ versus radius r. No dependence on the derivatives of $W(r)$ is included. Note expanded scale of α.

TABLE III. Estimates of parameters α, β^a, β^{na}, and γ by the Bates-Damgaard method.

	K$^-$($4p\epsilon s$)	Rb$^-$($5p\epsilon s$)	Cs$^-$($6p\epsilon s$)
α	6.00 (2)	8.40 (2)	1.46 (3)
β^a	1.96 (4)	3.24 (4)	9.73 (4)
β^{na}	3.92 (4)	6.48 (4)	1.95 (5)
γ	1.78 (6)	3.88 (6)	2.51 (7)

$$\alpha_\mu = 2 \sum_{\nu\neq\mu} \frac{|\bar{V}_{\mu\nu}|^2}{E_\nu - E_\mu},$$

$$\beta_\mu^a = \sum_{\nu\neq\mu} \frac{|\bar{V}_{\mu\nu}|^2}{(E_\nu - E_\mu)^2}[l_\nu(l_\nu+1) - l_\mu(l_\mu+1)],$$

$$\beta_\mu^{na} = 4 \sum_{\nu\neq\mu} \frac{|\bar{V}_{\mu\nu}|^2}{(E_\nu - E_\mu)^2}, \tag{A10}$$

$$\gamma_\mu = 8 \sum_{\nu\neq\mu} \frac{|\bar{V}_{\mu\nu}|^2}{(E_\nu - E_\mu)^3},$$

and the summation implies the averaging over the magnetic quantum number M_μ.

In special circumstances (e.g., for an isotropic atomic state), the sum $\beta^a + \beta^{na}$ reduces to the value 6β derived previously[17] by virtue of the properties of 3-j and 6-j symbols and $l_\nu = l_\mu \pm 1$. It is clear from Eq. (A8) that the energy-dependent term in the post-adiabatic theory is necessarily attractive provided that $E - E_\mu > 0$ and that E_μ is the ground-state energy of the residual atom. Our result for this term $-2(E-E_\mu)\gamma_\mu/2r^6$ differs from the corresponding quantity in Refs. 9 and 10 by the factor $-\frac{2}{3}$ (i.e., it differs in sign and magnitude). The values of these parameters are estimated using the Bates-Damgaard method in Table III.

---

[1] (a) J. Slater, F. H. Read, S. E. Novick, and W. C. Lineberger, Phys. Rev. A 17, 201 (1978), and references therein. (b) R. A. Falk, Ph.D. thesis, University of Washington, 1979 (unpublished).

[2] P. Frey, F. Breyer, and H. Hotop, J. Phys. B 11, L589 (1978).

[3] C. M. Lee, Phys. Rev. A 11, 1692 (1975).

[4] (a) D. W. Norcross and K. T. Taylor (unpublished). (b) D. L. Moores and D. W. Norcross, Phys. Rev. A 10, 1646 (1974).

[5] T. F. O'Malley, L. Spruch, and L. Rosenberg, J. Math. Phys. 2, 491 (1961).

[6] C. H. Greene, Phys. Rev. A 22, 149 (1980).

[7] T. F. O'Malley, JILA Report No. 14, 1964 (unpublished).

[8] C. H. Greene, U. Fano, and G. Strinati, Phys. Rev. A 19, 1485 (1979).

[9] M. J. Seaton and L. Steenman-Clark, J. Phys. B 10, 2639 (1977).

[10] R. J. Drachman, J. Phys. B 12, L699 (1979).

[11] L. Castillejo, I. C. Percival, and M. J. Seaton, Proc. R. Soc. London Ser. A 254, 259 (1960).

[12] E. Vogt and G. H. Wannier, Phys. Rev. 95, 1190 (1954).

[13] N. A. W. Holzwarth, J. Math. Phys. 14, 191 (1973).

[14] P. Morse and H. Feshbach, *Methods of Theoretical Physics* (McGraw-Hill, New York, 1953), p. 556. The correspondence between the notations in this reference and ours is $b = 2kf + (l+\frac{1}{2})^2$, $h^2 = 4kf$.

[15] This fact can be proven analytically using identities (13), (17), and (B12) of Ref. 13.

[16] L. M. Delves, Nucl. Phys. 9, 391 (1958–1959).

[17] (a) C. J. Kleinman, Y. Hahn, and L. Spruch, Phys. Rev. 165, 53 (1968); (b) O. Hinckelmann and L. Spruch, Phys. Rev. A 3, 692 (1971); (c) R. O. Berger, H. B. Snodgrass, and L. Spruch, Phys. Rev. A 5, 113 (1969).

[18] A. Dalgarno, G. W. F. Drake, and G. A. Victor, Phys. Rev. 176, 194 (1968).

[19] Here the term "adiabatic" means that the effect involves no variation in r, and conversely for the term "nonadiabatic." Thus the angular-momentum-dependent term $\beta^a/2r^6$ in Eq. (A9) is an adiabatic correction in our context.

[20] C. W. Clark, Phys. Rev. A 20, 1875 (1979).

[21] H. Klar and U. Fano, Phys. Rev. Lett. 37, 1134 (1976).

[22] H. Klar, Phys. Rev. A 15, 1452 (1977).

[23] See. Ref. 14, Eq. (9.1.36).

[24] U. Fano and G. Racah, *Irreducible Tensorial Sets* (Academic, New York, 1959). See Eq. (15.6).

[25] M. Rotenberg, R. Bivins, N. Metropolis, and J. K. Wooten, Jr., *The 3-j and 6-j Symbols* (Technology, Cambridge, Mass., 1959).

[26] I. I. Sobel'man, *An Introduction to the Theory of Atomic Spectra* (Pergamon, New York, 1972); see p. 342.